Available online at www.sciencedirect.com
SCIENCE DIRECT®
Journal of Power Sources 136 (2004) 10–15
JOURNAL OF POWER SOURCES
www.elsevier.com/locate/jpowsour

Methanol electrooxidation at Pt–Ru–W sputter deposited on Au substrate

Minoru Umeda [a], Hiroyuki Ojima [b], Mohamed Mohamedi [b,*], Isamu Uchida [b]

[a] *Department of Chemistry, Faculty of Engineering, Nagaoka University of Technology, Kamitomioka 1603-1, Nagaoka, Niigata 940-2188, Japan*
[b] *Department of Applied Chemistry, Graduate School of Engineering, Tohoku University, Aramaki-Aoba 07, Aoba-ku, Sendai 980-8579, Japan*

Received 19 March 2004; received in revised form 14 May 2004; accepted 14 May 2004

Available online 29 July 2004

Abstract

This work reports an improved electrocatalytic activity for methanol oxidation at Pt–Ru–W electrode sputter deposited on Au substrate. The performance of Pt–Ru–W was compared with that of Pt–W and of Pt–Ru alloy electrodes. All the alloys tested exhibited catalytic activity higher than Pt. Among the alloys tested, the Pt–Ru–W demonstrated a significant cathodic shift in the onset potential and a remarkable enhancement in the current density for methanol oxidation reaction (MOR). The onset potentials for the MOR matched well the anodic peak potentials recoded in the base electrolyte (H_2SO_4), i.e., 0.15 V versus Ag/AgCl for Pt–Ru–W and 0.35 V versus Ag/AgCl for Pt–W and Pt–Ru electrodes. From these findings, it was postulated that the background peak current generates oxide species necessary to complete the methanol oxidation to CO_2. Next, it was observed that the current density at Pt–Ru–W electrode decreased when the Au substrate was changed to Pt, C, or Si, although, the onset potential for MOR remained almost unaffected by the nature of the substrate. Afterwards, the effect of Au substrate on methanol oxidation at Au-based alloy electrodes was investigated.

Keywords: Methanol oxidation; Platinum; Ruthenium; Tungsten; Substrate effect

1. Introduction

The methanol oxidation reaction (MOR) is of great interest because of its potential application to direct methanol fuel cells (DMFCs) [1]. Hence, various electrocatalysts have been investigated in order to enhance the methanol oxidation [2–19]. One type of promotion of methanol electrooxidation is alloying platinum with another metal [20], where the second metal forms a surface oxide in the potential range for methanol oxidation. This is the basis for studies of alloying Pt with W [21–30], Sn [31–34], Mo [35–38], V [21,39], Cu [40–42]. Pt-based ternary systems were also considered [8,16,23,39]. The most active promoter known so far is ruthenium. The function of Ru was first suggested by Watanabe and Motoo [2], who proposed a bifunctional mechanism in which platinum dissociates methanol by chemisorption and the surface ruthenium atoms or islands acted as preferential sites for OH adsorption at low potentials. However, a low natural abundance of Ru is a drawback of this catalyst for practical uses.

It is generally accepted that the electrooxidation of methanol at binary alloys follows the so-called bifunctional mechanism [2,13]:

$$CO_2 + 6H^+ + 6e^- \Leftrightarrow CH_3OH + H_2O \quad (E^0 = 0.03\,\text{V versus NHE}) \tag{1}$$

$$Pt + CO \rightarrow Pt\text{–}CO_{ad} \tag{2}$$

$$M + H_2O \rightarrow M\text{–}OH_{ad} + H^+ + e^- \quad (M = Ru, Sn, W, Mo, \ldots) \tag{3}$$

$$Pt\text{–}CO_{ad} + M\text{–}OH_{ad} \rightarrow CO_2 + Pt + M + H^+ + e^- \tag{4}$$

However, little is known about methanol oxidation mechanism at ternary alloys or on the interaction between the catalyst and the support material [43,44].

Here we report a remarkable promotion of methanol electrooxidation at Pt–Ru–W electrode. The Pt–Ru–W layer was sputter-deposited on a gold substrate and its performance was compared with that of binary systems such as Pt–W and Pt–Ru. The effect of the material substrate was also

* Corresponding author. Present address: Institut National de la Recherche Scientifique (INRS), University of Quebec, Centre Énergie, Matériaux et Télécommunications 1650, boul. Lionel Boulet, Varennes, Québec, Canada J3X 1S2. Tel.: +1 450 929 8231; fax: +1 450 929 8102.
E-mail address: mohamedi@inrs-emt.uquebec.ca (M. Mohamedi).

0378-7753/$ – see front matter © 2004 Elsevier B.V. All rights reserved.
doi:10.1016/j.jpowsour.2004.05.013

investigated by considering other material than gold such as platinum, silicone, and carbon.

2. Experimental

The electrode catalyst consisted of 0.3 μm-thick layer prepared by sputter-deposition on both sides of an Au flag substrate of 5 mm-diameter and 0.3 mm thick. Pt, Si and glassy carbon (Tokai Carbon) were also used as substrate for comparison. The deposition was performed with a multi-sputter-target machine (Anelva, L-350S-C). The chamber was evacuated to a base pressure of 10^{-4} Pa. The deposition was carried out at 300 °C in the chamber filled with 99.999% pure Argon gas to 10 Pa under a substrate rotation speed of 20 rpm.

Elemental analysis of thus sputter-deposited layer was conducted by using an X-ray fluorescence spectrometer (Seiko Instruments, SEA5120). The phase structure was analyzed with an X-ray diffractometer (Shimadzu, XD-D1) using Cu Ka radiation.

The electrochemical measurements were carried out in a deaerated solution of 0.5 M H_2SO_4 + 1 M CH_3OH. A Pt coil and an Ag/AgCl were used as counter and reference electrodes, respectively. Current–potential (*I–E*) curves were measured by a potentiostat (Hokuto Denko, HA 1010). Prior to electrochemical measurements in methanol containing solution, the surface of the working electrode was cleaned electrochemically by potential cycling in 0.5 M H_2SO_4. All the electrochemical measurements were carried out at 23 ± 0.5 °C. The real surface area being impossible to determine for the alloys, the current densities are thus referred to the geometric surface area of the electrodes.

3. Results and discussion

3.1. Characterization of the sputter-deposited electrodes

The desired composition of either the binary or ternary elements was obtained after optimization of the sputtering conditions; this was achieved by performing several experimental trials following the OVAT (one variable at time) protocol. The parameters that were found to decide on the composition were the substrate temperature, the individual targets power, and the sputtering time. Besides X-ray fluorescence, the elemental composition was always verified by EDX, and ICP.

The XRD patterns of the sputtered binary and ternary metal catalysts are given in Fig. 1, where each diffraction peak was indexed by calculating an interplanar spacing [45]. Compositions of the binary and ternary alloys determined by elemental analysis are also indicated in the figure. In Fig. 1, diffraction patterns marked with black dots correspond to the gold substrate. In Fig. 1(a), the diffraction peaks based on Pt are of fcc crystalline structure.

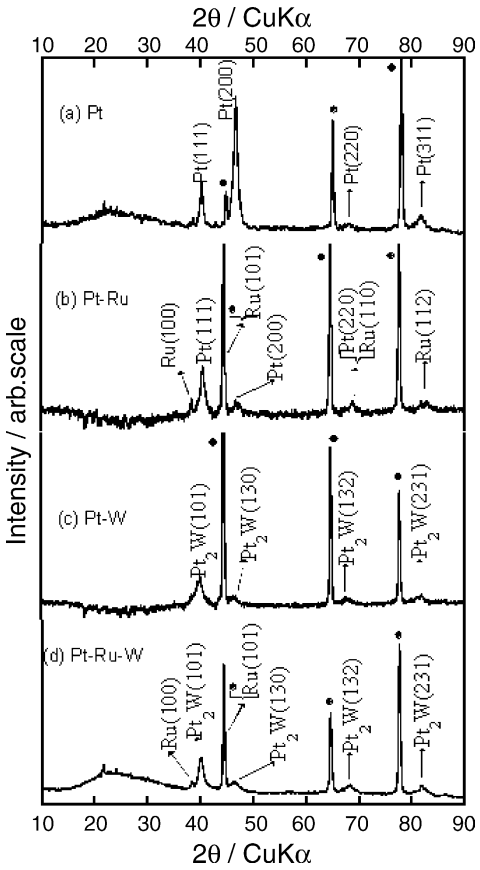

Fig. 1. XRD analysis of Pt-based sputtered layer prepared on Au substrate: (a) Pt, (b) $Pt_{80}Ru_{20}$, (c) $Pt_{85}W_{15}$, (d) $Pt_{65}Ru_{20}W_{15}$. Dot-marked peaks originate from the Au substrate.

XRD pattern for Pt–Ru alloy (Fig. 1(b)) showed diffraction angles almost similar to those of sputtered Pt, although, the peak angles slightly shifted from those of Pt or Ru alone [46]. The observed peak intensity of Pt is much higher than that of Ru, which indicates that Ru dissolves in Pt to form a Pt–Ru alloy of Pt (fcc) crystalline structure.

XRD pattern of Pt–W shown in Fig. 1(c), revealed peaks belonging to Pt_2W of rhombic structure. It has been reported that in case where W content is small, two intermediate phases of γ(Pt_2W) and ε(PtW) are formed below 1400 °C [47]. Accordingly, the $Pt_{85}W_{15}$ is considered to be γ phase in which Pt content is comparatively high.

Fig. 1(d) represents XRD pattern of Pt–Ru–W alloy. Besides, the peaks related to the Pt_2W rhombic structure, another part of the peaks is reverted to Ru (hcp) crystalline structure. The diffraction peak intensity of the former is greater than that of the latter. The deposited Pt–Ru–W is thus characterized as a Ru-dissolved Pt_2W rhombic structure.

3.2. Characterization of methanol oxidation at Pt-based alloy electrodes by voltammetry

Fig. 2 shows the results of linear sweep voltammograms experiments with different Pt and Pt-based alloy catalysts.

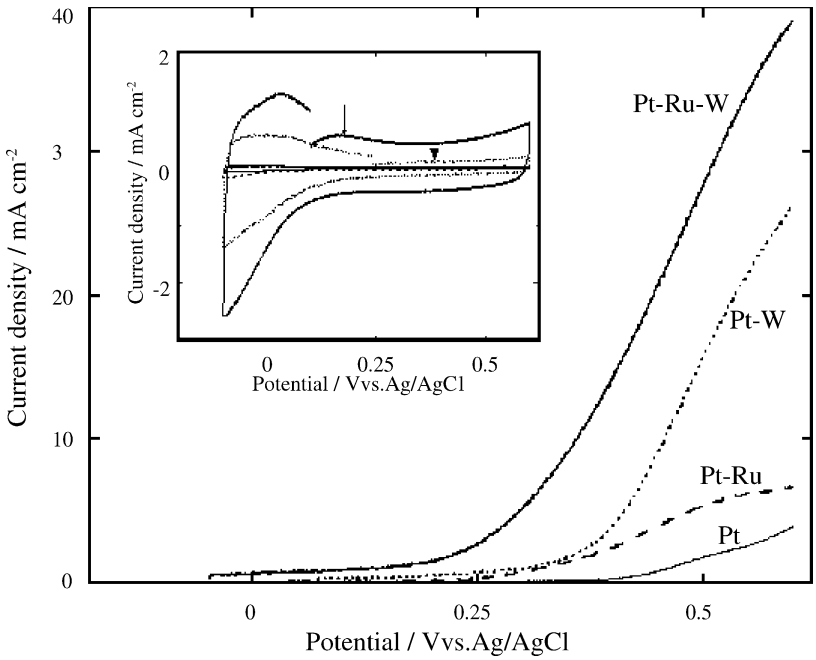

Fig. 2. Linear sweep voltammograms at $Pt_{65}Ru_{20}W_{15}$ (solid line), $Pt_{85}W_{15}$ (dotted line), $Pt_{80}Ru_{20}$ (dashed line), and Pt (thin solid line) all sputtered on Au substrate measured in 0.5 M H_2SO_4 + 1 M CH_3OH. Inset shows background CVs of the corresponding electrodes in 0.5 M H_2SO_4 solution. Sweep rate: 10 mV s^{-1}.

The experiments were conducted at room temperature in 0.5 M H_2SO_4 + 1 M CH_3OH solution with 10 mV s^{-1}. As expected at Pt–Ru electrode, methanol oxidation potential is shifted towards cathodic values and higher current densities are observed when compared to Pt electrode. These phenomena are well explained by the bifunctional mechanism proposed by Watanabe and Motoo [2]. Similar observations can be made with Pt–W and Pt–Ru–W alloys, with the latter exhibiting a remarkable enhancement both in terms of current density and cathodic shift in the oxidation potential.

Attempt can be made to explain the above results by considering the bifunctional mechanism; the onset potential is attributed to an electrode potential that causes reaction (3) to occur. Therefore, the following thermodynamic data provide the onset potential of methanol oxidation at Pt-based electrodes

$$PtO + 2H^+ + 2e^- \Leftrightarrow Pt + H_2O \quad (E^0 = 0.98\,\text{V versus NHE}) \tag{5}$$

$$Ru_2O_3 + 6H^+ + 6e^- \Leftrightarrow 2Ru + 3H_2O \quad (E^0 = 0.74\,\text{V versus NHE}) \tag{6}$$

$$WO_2 + 4H^+ + 4e^- \Leftrightarrow W + 2H_2O \quad (E^0 = -0.12\,\text{V versus NHE}) \tag{7}$$

$$W_2O_5 + 2H^+ + 2e^- \Leftrightarrow 2WO_2 + H_2O \quad (E^0 = -0.03\,\text{V versus NHE}) \tag{8}$$

$$2WO_3 + 2H^+ + 2e^- \Leftrightarrow W_2O_5 + H_2O \quad (E^0 = 0.09\,\text{V versus NHE}) \tag{9}$$

It seems thus possible by using these materials to reduce the electrode potential of methanol oxidation to the standard potential given in Eq. (1).

The cyclic voltammograms for Pt as well as for Pt-based alloys recorded in a deaerated 0.5 M H_2SO_4 solution are shown as inset in Fig. 2. Anodic current peaks are seen at ca. 0.15 V versus Ag/AgCl for Pt–Ru–W electrode (indicated by arrow) and around 0.3–0.35 V versus Ag/AgCl for Pt–Ru and Pt–W electrodes (indicated by arrow head). In terms of current densities, the order of activities is Pt–Ru–W > Pt–W > Pt–Ru. Accordingly, the onset potential for methanol oxidation (Fig. 2) correlates well with the anodic peak in the base electrolyte (Fig. 2, inset).

Differential electrochemical mass spectroscopy (DEMS) study revealed that CO_2 production occurred at the onset potential of methanol electrooxidation, whereas the oxide formation by water decomposition is the rate determining [7,48]. If one assumes that the anodic current peaks in the base electrolyte (inset of Fig. 2) represent the adsorption of OH, then the methanol oxidation current following the background peak could be explained based on Eq. (4). Thus, the mechanism in which the Pt–Ru–W exhibits higher methanol-oxidation activity in terms of onset potential is attributed to the most cathodic potential for OH adsorption.

Since the binary and ternary electrodes are in alloy forms, $M–OH_{ad}$ formation does not always proceed according to the thermodynamic data given in Eqs. (6)–(9). However, Pt–Ru–W electrode facilitates the generation of $M–OH_{ad}$ more than Pt–Ru or Pt–W. It is likely that the Ru-dissolved in the Pt_2W phase easily brings about the W/WO_x reaction rather than Pt_2W alloy.

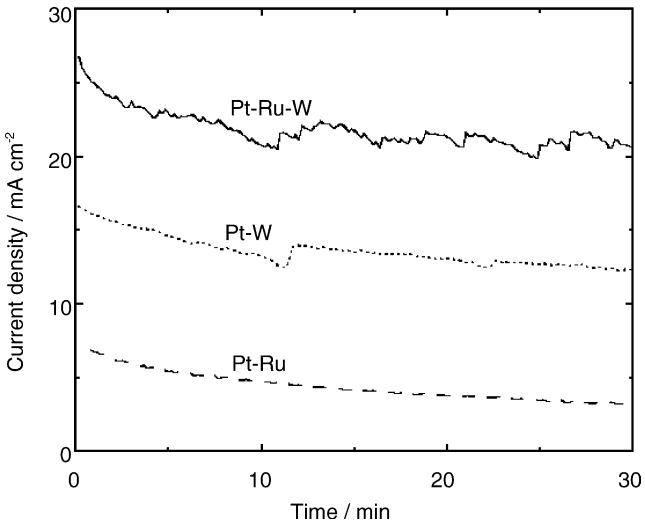

Fig. 3. Current density versus time curves at $Pt_{65}Ru_{20}W_{15}$ (solid line), $Pt_{85}W_{15}$ (dotted line) and $Pt_{80}Ru_{20}$ (dashed line) sputtered on Au substrate measured in 0.5 M H_2SO_4 + 1 M CH_3OH. The potential was stepped from the rest potential to 0.5 V vs. Ag/AgCl.

3.3. Stationary potential electrolysis

The Pt–Ru, Pt–W and Pt–Ru–W electrodes were subjected to stationary potential electrolysis at 0.5 V versus Ag/AgCl for 30 min. The experimental *I–t* curves are shown in Fig. 3. The Pt–Ru–W electrode demonstrated the highest current density in agreement with the voltammetric observations of Fig. 2. In Fig. 3, the current densities at Pt–Ru–W and Pt–W electrodes are unstable in the early stage; however, they are gradually stabilized at 80% of their initial values. On the other hand, the current density at Pt–Ru decreased to one half of its initial value after 30 min of electrolysis. Consequently, Pt–Ru–W deposited on Au electrode demonstrated an extreme catalytic activity, in terms of both onset potential and current density towards methanol oxidation.

3.4. Effect of the material substrate

Fig. 4 shows *I–E* curves for methanol oxidation at Pt–Ru–W, Pt–W and Pt–Ru electrodes prepared on various substrates, namely, Au, Pt, Si and C. Insets represent the CVs in the base electrolyte. A remarkable effect of the substrate can be noticed depending on the nature of the alloy. For the Pt–Ru–W (Fig. 4(A)), methanol oxidation current density decreased when the Au substrate was changed to Pt, C, or Si, although, the onset potential remained almost unaffected by the nature of the substrate. This implies that the use of Au as a substrate accelerates CO_2 evolution according to reaction (4). Thus, the mechanism based on Au substrate would be considered to have enhanced the OH adsorption quantitatively in reaction (3). This can be understood by looking at the background CVs in the inset of Fig. 4(A), where the magnitude of the background current peak at ca. 0.15 V versus Ag/AgCl, which is believed to produce $M–OH_{ad}$, is the highest for electrodes using Au substrate. Consequently, the use of Au substrate for Pt–Ru–W improved the OH adsorption quantitatively.

In the case of Pt–W (Fig. 4(B)), the methanol oxidation *I–E* curves are not influenced by the nature of the substrate. This is because no change in the background CV has occurred (inset of Fig. 4(B)). On the contrary, for Pt–Ru alloy, the use of Au substrate obviously diminished the methanol-oxidation current as shown in Fig. 4(C). The magnitude of the background currents (inset of Fig. 4(C)) are in the order of Pt > Si > Au substrate, which is of similar trend as for the methanol oxidation current. Therefore, in the case of Pt–Ru, the substrate material affects the quantity of $M–OH_{ad}$ formed or the effective electrode area.

Quite the opposite is observed on the effect of the substrate type onto the onset potential of methanol oxidation. Indeed, Fig. 4 shows that methanol oxidation is solely dependent on the kind of Pt-based electrocatalyst. Among the combinations tried here, i.e., substrate nature, and electrocatalysts,

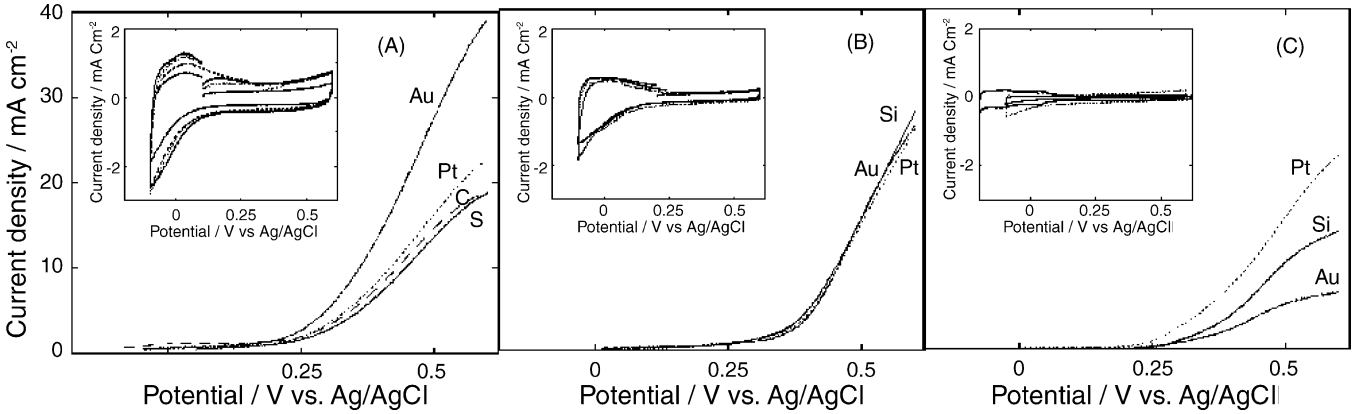

Fig. 4. Linear sweep voltammograms at (A) $Pt_{65}Ru_{20}W_{15}$, (B) $Pt_{85}W_{15}$ and (C) $Pt_{80}Ru_{20}$ deposited on different substrates: Au (solid line), Pt (dotted line), Si (thin solid line), C (dashed line) measured in 0.5 M H_2SO_4 + 1 M CH_3OH. Inset shows background CVs of the corresponding electrodes in 0.5 M H_2SO_4 solution. Sweep rate: 10 mV s^{-1}.

Pt–Ru–W sputter-deposited on Au substrate seems to be the most active one towards methanol oxidation.

The role of the gold substrate may be considered by looking at the following electrode reaction:

$$Au_2O_3 + 6H^+ + 6e^- \Leftrightarrow 2Au + 3H_2O \quad (E^0 = 1.457\,V) \tag{10}$$

This reaction points out that a direct participation of Au to form M–OH_{ad} is unlikely to occur. Therefore, the Au substrate is presumed to affect indirectly the number of M–OH_{ad} formed on the Pt–Ru–W surface to complete the methanol oxidation.

In order to further investigate the function of Au, Au-based binary and Au-based ternary systems were prepared on Au substrate. Fig. 5 illustrates voltammetry carried out at these electrodes in both methanol aqueous solution and in 0.5 M H_2SO_4 solution. It can be seen that methanol oxidation current densities obtained at Pt–Ru–Au and Pt–W–Au electrodes do not exceed these recorded at Pt–Ru–W electrode. In addition, the background CVs of Pt–Ru–Au and Pt–W–Au electrodes (inset of Fig. 5), do not exhibit current originating from oxide species at ca. 0.15–0.35 V versus Ag/AgCl. This explains the low activity of these electrodes to complete the methanol oxidation. These results confirm that Au is not responsible for the cathodic shift in the MOR onset potential. Fig. 6 shows CVs run at Ru–Au and W–Au electrodes in an electrolytic solution with and without methanol. No electrocatalytic towards methanol oxidation activity is recorded with these two electrodes at the room temperature condition. Au without being combined to Pt does not exhibit any catalytic activity for methanol oxidation. The recent work of Waszczuk et al.

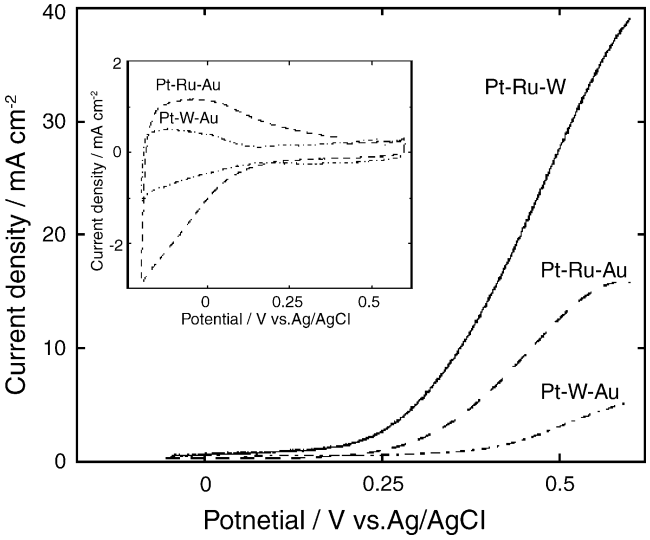

Fig. 5. Linear sweep voltammograms at $Pt_{65}Ru_{20}Au_{15}$ (dashed line) and $Pt_{70}W_{20}Au_{10}$ (dash-dotted line) sputtered on Au substrate measured in 0.5 M H_2SO_4 + 1 M CH_3OH. Inset shows background CVs of the corresponding electrodes in 0.5 M H_2SO_4 solution. LSV at $Pt_{65}Ru_{20}W_{15}$ is also reported for comparison. Sweep rate: 10 mV s^{-1}.

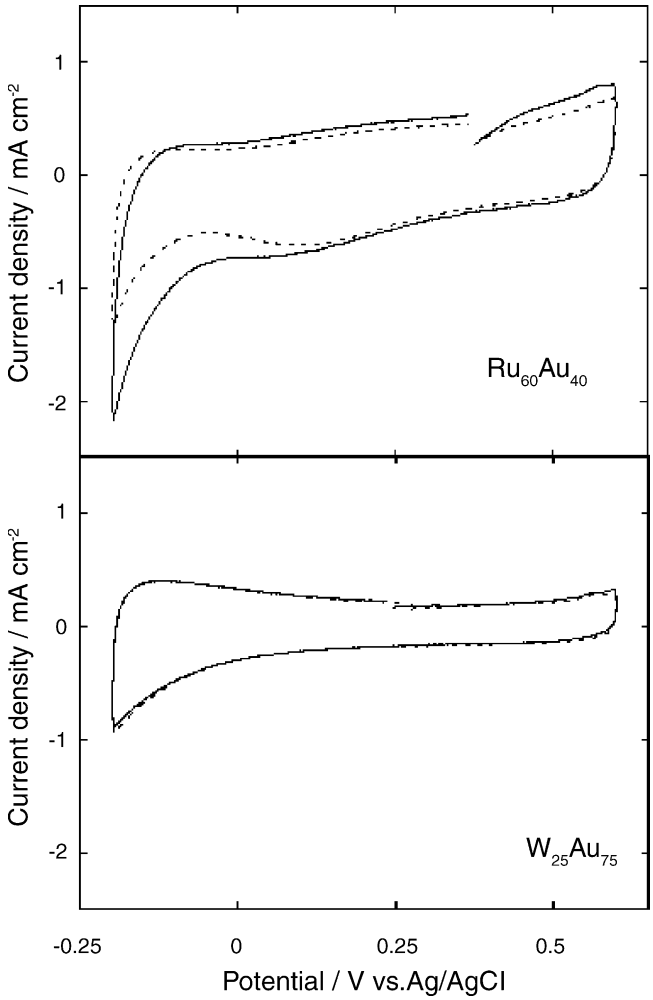

Fig. 6. Cyclic voltammograms at $Ru_{60}Au_{40}$ (upper) and $W_{25}Au_{75}$ (lower) sputtered on Au substrate measured in 0.5 M H_2SO_4 + 1 M CH_3OH. Dashed curves are background CVs. Sweep rate: 10 mV s^{-1}.

[5], suggests a combination of both bifunctional and ligand (electronic) effects that causes the carbon monoxide desorption. It is likely that Au substrate electronically affects the Pt–Ru–W surface in terms of M–OH_{ad} creation.

4. Conclusions

In summary, a remarkable promotion of methanol electrooxidation at Pt–Ru–W sputter deposited on Au substrate is reported here. First, the performance of Pt–Ru–W was compared with that of Pt–W and of Pt–Ru, both exhibiting catalytic activity greater than Pt. Compared to the binary alloys, higher current densities and a noticeable cathodic shift in the onset potential for methanol oxidation was observed at Pt–Ru–W electrode. The onset potentials for MOR coincided with the anodic peak potentials recoded in the base electrolyte: 0.15 V versus Ag/AgCl for Pt–Ru–W and 0.35 V versus Ag/AgCl for Pt–W and Pt–Ru. Accordingly, it is postulated that the background peak current generates oxide

species required to complete the oxidation of methanol to CO_2. Finally, stationary potential electrolysis confirmed that the Pt–Ru–W prepared on Au exhibits the highest activity towards methanol oxidation.

Next, by replacing the Au substrate with Pt, Si and C, only a decrease in the current density was observed at Pt–Ru–W deposited electrode. The experimental result, in which only a change in the magnitude of background peak current at 0.15 V versus Ag/AgCl was observed, strongly suggests that the Au substrate quantitatively influences the number of oxide species formed on the electrode.

Acknowledgements

The present work was supported by Grant-in-Aids for Scientific Research (B) (No. 14350450) from the Ministry of Education, Culture, Sports, Science and Technology, Japan.

References

[1] S. Wasmus, A. Küver, J. Electroanal. Chem. 461 (1999) 14.
[2] M. Watanabe, S. Motoo, J. Electroanal. Chem. 60 (1975) 267.
[3] A. Kabbabi, R. Faure, R. Durand, B. Beden, F. Hahn, J.-M. Léger, C. Lamy, J. Electroanal. Chem. 444 (1998) 41.
[4] J.-M. Léger, J. Appl. Electrochem. 31 (2001) 767.
[5] P. Waszczuk, A. Wieckowski, P. Zelenay, S. Gottesfeld, C. Coutanceau, J.-M. Léger, C. Lamy, J. Electroanal. Chem. 511 (2001) 55.
[6] K. Wang, H.A. Gasteiger, N.M. Markoviæ, P.N. Ross, Electrochim. Acta 41 (1996) 2587.
[7] H. Wang, C. Wingender, H. Baltruschat, M. Lopez, M.T. Reetz, J. Electroanal. Chem. 509 (2001) 163.
[8] K.L. Ley, R. Liu, C. Pu, Q. Fan, N. Leyarovska, C. Segre, E.S. Smotkin, J. Electrochem. Soc. 144 (1997) 1543.
[9] P. Waszczuk, G.-Q. Lu, A. Wieckowski, C. Lu, C. Rice, R.I. Masel, Electrochim. Acta 47 (2002) 3637.
[10] S. Wasmus, A. Kuver, J. Electroanal. Chem. 461 (1999) 14.
[11] A. Hamnett, Catal. Today 38 (1997) 445.
[12] K. Ota, Y. Nakagawa, M. Takahashi, J. Electroanal. Chem. 179 (1984) 179.
[13] H.A. Gasteiger, N. Markoviæ, P.N. Ross Jr., E.J. Cairns, Electrochim. Acta 39 (1994) 1825.
[14] N.M. Markoviæ, H.A. Gasteiger, P.N. Ross Jr., J. Jiang, I. Villegas, M.J. Weaver, Electrochim. Acta 40 (1995) 91.
[15] A.V. Tripkovic, K.Dj. Popovic, J.D. Lovic, Electrochim. Acta 46 (2001) 3163.
[16] C. Lamy, A. Lima, V. LeRhun, F. Delime, C. Coutanceau, J.-M. Léger, J. Power Sour. 105 (2002) 283.
[17] M. Umeda, M. Mohamedi, I. Uchida, Langmuir 17 (2001) 7970.
[18] K. Lasch, G. Hayn, L. Jörissen, J. Garche, O. Besenhardt, J. Power Sour. 105 (2002) 305.
[19] C.-G. Lee, T. Itoh, M. Mohamedi, M. Umeda, I. Uchida, H.-C. Lim, Electrochemistry 71 (2003) 549.
[20] A. Hamnett, in: A. Wieckowski (Ed.), Interfacial Electrochemistry: Theory, Experimental and Applications, Marcel Dekker, New York, 1999.
[21] A. Lima, C. Coutanceau, J.M. Léger, C. Lamy, J. Appl. Electrochem. 31 (2001) 379.
[22] M. Gotz, H. Wendt, Electrochim. Acta 43 (1998) 3637.
[23] A.S. Arico, Z. Poltarzewski, H. Kim, A. Morana, N. Giordano, V. Antonucci, J. Power Sour. 55 (1995) 159.
[24] A.S. Arico, P. Creti, N. Giordano, V. Amtpmicci, J. Appl. Electrochem. 26 (1996) 959.
[25] C. He, H.R. Kunz, J.M. Fenton, in: Electrochemical Society Proceedings, PV 97-13, Pennington, NJ, 1997, p. 52.
[26] P.K. Shen, A.C.C. Tseung, J. Electrochem. Soc. 141 (1994) 3082.
[27] P. Shen, K. Chen, A.C.C. Tseung, J. Chem. Soc., Faraday Trans. 90 (1994) 3089.
[28] A. Gamnett, B.J. Kennedy, S.A. Weeks, J. Electroanal. Chem. 240 (1988) 349.
[29] A.C.C. Tseung, K.Y. Chen, Catal. Today 38 (1997) 439.
[30] P.J. Kulesza, L.R. Faulkner, J. Electroanal. Chem. 259 (1989) 81.
[31] M. Krausa, W. Vielstich, J. Electroanal. Chem. 379 (1994) 307.
[32] T. Frelink, W. Visscher, A.P. Cox, J.A.R. Van Veen, Electrochim. Acta 40 (1995) 1537.
[33] S.C. Gebhard, R.G. Windham, B.E. Koel, J. Phys. Chem. 94 (1990) 6831.
[34] Y. Ishikawa, M. Liao, C.R. Cabrera, Surf. Sci. 463 (2000) 66.
[35] S. Mukerjee, S.J. Lee, E.A. Ticianelli, J. McBreen, B.N. Grgur, N.M. Markoviæ, P.N. Ross, J.R. Giallombardo, E.S. De Castro, Electrochem. Solid-State Lett. 2 (1999) 12.
[36] G. Samjeske, H. Wang, T. Löffer, H. Baltruschat, Electrochim. Acta 47 (2002) 3681.
[37] B.N. Grgur, G. Zhuang, N.M. Markoviæ, P.N. Ross, J. Phys. Chem. B 101 (1997) 3910.
[38] B.N. Grgur, N.M. Markoviæ, P.N. Ross, J. Phys. Chem. B 102 (1998) 2494.
[39] K. Lasch, L. Jorissen, J. Garche, J. Power Sour. 84 (1999) 225.
[40] N. Markoviæ, P.N. Ross, J. Electroanal. Chem. 330 (1992) 499.
[41] W. Yang, D. Jaramillo, J.J. Gooding, D.B. Hibbert, R. Zhang, G.D. Willett, J. Fisher, Chem. Commun. (2001) 1982.
[42] I. Rubinstein, S. Steinberg, Y. Tor, A. Shanzer, J. Sagiv, Nature 332 (1988) 31.
[43] P.L. Antonucci, V. Alderucci, N. Giordano, D.L. Cocke, H. Kim, J. Appl. Electrochem. 24 (1994) 58.
[44] M. Umeda, M. Kokubo, M. Mohamedi, I. Uchida, Electrochim. Acta 48 (2003) 1367.
[45] A.R. West, Basic Solid State Chemistry, Wiley, Tokyo, 1996.
[46] E. Antolini, F. Cardelloni, J. Alloys Compd. 313 (2001) 118.
[47] S. Nagasaki, M. Hirabayashi, Binary Alloy Phase Diagrams, AGNE, Tokyo, 2001.
[48] H. Wang, T. Löffler, H. Baltruschat, J. Appl. Electrochem. 31 (2001) 759.